Molecular Biology of the Cell
Vol. 18, 2561–2568, July 2007

Coordination of Hpr1 and Ubiquitin Binding by the UBA Domain of the mRNA Export Factor Mex67[D]

Maria Hobeika,* Christoph Brockmann,† Nahid Iglesias,‡ Carole Gwizdek,* David Neuhaus,† Françoise Stutz,‡ Murray Stewart,† Gilles Divita,§ and Catherine Dargemont*

*Institut Jacques Monod, Universités Paris VI and VII, Centre National de la Recherche Scientifique, 75251 Paris Cedex 05, France; †Medical Research Council Laboratory of Molecular Biology, Cambridge CB2 2QH, United Kingdom; ‡Department of Cell Biology, Sciences III, 1211 Geneva 4, Switzerland; and §Centre de Recherches de Biochimie Macromoléculaire, Centre National de la Recherche Scientifique Formation de Recherche en Evolution-2593, Molecular Biophysics and Therapeutics, 34293 Montpellier Cedex 5, France

Submitted February 20, 2007; Revised April 18, 2007; Accepted April 23, 2007
Monitoring Editor: Thomas Sommer

The ubiquitin-associated (UBA) domain of the mRNA nuclear export receptor Mex67 helps in coordinating transcription elongation and nuclear export by interacting both with ubiquitin conjugates and specific targets, such as Hpr1, a component of the THO complex. Here, we analyzed substrate specificity and ubiquitin selectivity of the Mex67 UBA domain. UBA-Mex67 is formed by three helices arranged in a classical UBA fold plus a fourth helix, H4. Deletion or mutation of helix H4 strengthens the interaction between UBA-Mex67 and ubiquitin, but it decreases its affinity for Hpr1. Interaction with Hpr1 is required for Mex67 UBA domain to bind polyubiquitin, possibly by inducing an H4-dependent conformational change. In vivo, deletion of helix H4 reduces cotranscriptional recruitment of Mex67 on activated genes, and it also shows an mRNA export defect. Based on these results, we propose that H4 functions as a molecular switch that coordinates the interaction of Mex67 with ubiquitin bound to specific substrates, defines the selectivity of the Mex67 UBA domain for polyubiquitin, and prevents its binding to nonspecific substrates.

INTRODUCTION

Ubiquitylation has emerged as a major regulatory mechanism for highly diverse cellular functions. Ubiquitin can be conjugated to its target as a monomer or a polyubiquitin chain that can be linked through several different lysine residues. Polyubiquitin chains linked by Lys48 promote proteasome-dependent degradation of target proteins, whereas monoubiquitination or Lys63-linked polyubiquitin is involved in the nonproteolytic regulation of various functions such as vesicular transport or DNA repair (Pickart and Eddins, 2004).

The diverse functions generated by different ubiquitin modifications are mediated through effector proteins that contain ubiquitin binding motifs that can be classified into six major groups according to their precise structural fold (for reviews, see Hicke *et al.*, 2005; Harper and Schulman, 2006). Crystallography and nuclear magnetic resonance (NMR) have shown that, although they show relatively low sequence conservation, three of these domains, "ubiquitin associated" (UBA), "coupling of ubiquitin conjugation to endoplasmic reticulum" (CUE), and "GGA and Tom1" (GAT), adopt a compact helical fold consisting in three α-helices connected by two short loops that generates a large hydrophobic surface, mainly constituted by the C terminus of the helix 1, loop 1, and helix 3, which forms the principal interface with ubiquitin (for review, see Harper and Schulman, 2006). Lys63-linked polyubiquitins interact with UBA domains in a 1:1 stoichiometry, whereas with Lys48-linked diubiquitin, a single UBA domain binds both ubiquitins (Varadan *et al.*, 2004; Trempe *et al.*, 2005; Varadan *et al.*, 2005). A recent analysis of the ubiquitin binding properties of >25 UBA domains defined four classes of UBA domains ranging from no interaction, recognition of linkage-specific chains, to binding of both mono- and polyubiquitin (Raasi *et al.*, 2005), leading to the proposal that non-UBA sequences present in full-length proteins could modulate the interactions of a given UBA domain.

In *Saccharomyces cerevisiae*, two ubiquitin ligases, Tom1 and Rsp5, are involved in the regulation of poly(A)+ RNA nuclear export (Duncan *et al.*, 2000; Neumann *et al.*, 2003; Rodriguez *et al.*, 2003). The stability of Hpr1 (a component of the THO/TREX complex that couples transcription elongation to mRNA nuclear export) is modulated by the ubiquitin/proteasome pathway in an Rsp5-dependent manner (Gwizdek *et al.*, 2005). Mature yeast messenger ribonucleoproteins (mRNPs) are exported through nuclear pores by the Mex67:Mtr2 heterodimer (TAP:p15 in metazoans). Mex67:Mtr2 is recruited to mRNAs through RNA binding adaptors, including components of the THO/TREX complex (Rodriguez *et al.*, 2004). TAP has a modular structure that includes a 70-residue C-terminal domain with three helices arranged in a classical UBA fold plus an additional fourth helix (Liker *et al.*,

This article was published online ahead of print in *MBC in Press* (http://www.molbiolcell.org/cgi/doi/10.1091/mbc.E07–02–0153) on May 2, 2007.

[D] The online version of this article contains supplemental material at *MBC Online* (http://www.molbiolcell.org).

Address correspondence to: C. Dargemont (dargemont@ijm.jussieu.fr).

2000; Grant *et al*., 2002; Grant *et al*., 2003). We recently showed that Mex67 can interact with ubiquitin and polyubiquitylated proteins both in vitro and in vivo through its UBA domain (Gwizdek *et al*., 2006). Surprisingly, this UBA domain also interacts with specific partners, including Hpr1. This interaction gives ubiquitylated Hpr1 transient protection from proteosomal degradation. In addition to its mRNP nuclear export function, the Mex67 UBA domain also contributes to the recruitment of Mex67 to transcribing genes, possibly through its interaction with Hpr1. Altering ubiquitylation of Hpr1 affects these UBA-dependent functions of Mex67 (Gwizdek *et al*., 2006).

Here, we examine the basis for the interaction of the Mex67 UBA domain with both ubiquitin and Hpr1. Our in vitro and in vivo data show that helix H4 influences these interactions and suggest a model in which the affinity of the Mex67 UBA domain for ubiquitin is enhanced through a conformational change induced by its binding to Hpr1.

MATERIALS AND METHODS

Plasmids and Cloning

Plasmid constructs encoding the 57-amino acid (543–599) UBA domain of Mex67 and the 57 amino acid (342–398) UBA domain of Rad23 fused to glutathione S-transferase (GST) or LexA were described previously (Gwizdek *et al*., 2006). The DNA fragment encoding amino acids 543–589 of the UBA domain of Mex67 (UBAΔH4-Mex67) was amplified by polymerase chain reaction (PCR) by using pGEX-4T-1-UBA-Mex67 as a template, and it was cloned as a BamHI–SalI fragment into pGEX4T-1 and pLex10 vector (Invitrogen, Carlsbad, CA) to generate plasmids encoding GST-UBAΔH4-Mex67 and lexA-UBAΔH4-Mex67, respectively. A NcoI–NotI DNA fragment encoding amino acids 527–589 of Mex67 was amplified by PCR and cloned into the same restriction sites of pGex4T-1-Mex67 to obtain the pGex4T-1-Mex67ΔH4 (1-589) construct. Mutations of Phe596 and Val597 into Ala were introduced using the QuikChange II XL site-directed mutagenesis kit (Stratagene, La Jolla, CA). pRS314-Mex67-ΔH4-3HA was generated as described previously for pRS314-Mex67-3HA by using a EcoNI–NheI DNA fragment encoding amino acids 494–589 of Mex67. The plasmid was transformed into the MEX67 shuffle strain (Strasser *et al*., 2000) before selection on 5-fluoroorotic acid plates. Expression levels of Mex67-3HA and Mex67-ΔH4-3HA in the shuffled strains analyzed by Western blotting with anti-hemagglutinin (HA) antibodies were found to be similar.

Protein Purification

Recombinant proteins were expressed in *Escherichia coli* BL21(DE3). Strains transformed with pGEX4T-1-Mex67, pGEX4T-1-Mex67ΔUBA, or pGEX4T-1-Mex67ΔH4 were grown at 37°C up to OD_{600} = 0.6. Protein expression was then induced for 48 h at 18°C with 0.5 mM isopropyl β-D-thiogalactoside (IPTG) after cold and chemical shocks. GST-UBA-Mex67 and GST-UBA-Rad23 fusion proteins were expressed and induced as described previously (Gwizdek *et al*., 2006). GST-UBA-Mex67 was cleaved with thrombin before nuclear magnetic resonance (NMR) analysis. GST-UBAΔH4-Mex67 or His-UBA-Mex67 were expressed in *E. coli* grown at 37°C to an OD_{600} of 0.6 and induced with 0.5 mM IPTG for 24 h at 23°C. GST- or His-fusion proteins were then purified on glutathione-Sepharose 4B beads (GE Healthcare, Little Chalfont, Buckinghamshire, United Kingdom) or nickel-agarose beads (QIAGEN, Hilden, Germany), respectively, according to the manufacturer's instructions in the presence of 0.1% Triton X-100. The His-UBA-Mex67/GST-Hpr1 complex was formed by mixing purified recombinant His-UBA-Mex67 and GST-Hpr1 (Gwizdek *et al*., 2005) proteins followed by overnight dialysis at 4°C against 50 mM Tris, pH 7.5, 150 mM NaCl, and 10% glycerol and purification on glutathione-Sepharose beads.

Solution Structure of the Mex67 UBA Domain

NMR-spectra were acquired at 27°C on a Bruker Avance 500 spectrometer equipped with triple resonance cryoprobe. All experiments were performed on a uniformly ^{15}N- and ^{13}C-labeled sample containing 0.55 mM protein, 25 mM NaH_2PO_4, and 50 mM NaCl at pH 7.4 in 90% H_2O, 10% D_2O. All spectra were processed using the program XWINNMR (Bruker BioSpin, Rheinstetten, Germany). Backbone resonance assignment was carried out using the pair of triple resonance experiments CBCA(CO)NH/CBCANH (Grzesiek and Bax, 1992a,b). Side-chain resonances were identified using HBHA(CO)NH, HCCH-total correlation spectroscopy (TOCSY), and HCCH-correlation spectroscopy (COSY) (Kay *et al*., 2002) experiments. Interproton distance information for structure calculation was derived from a ^{15}N-nuclear Overhauser effect spectroscopy (NOESY)-heteronuclear single quantum correlation (HSQC) spectrum and a pair of ^{13}C-NOESY-HSQC spectra recorded for both aliphatic and aromatic resonances (Clore and Gronenborn, 1992). All NOESY spectra were acquired using a mixing time of 100 ms. The program CCPNMR Analysis (Vranken *et al*., 2005; Hajduk *et al*., 1997) was used for resonance assignment of the protein.

Secondary structure predictions were made using the chemical shift-based dihedral angle prediction software TALOS (Cornilescu *et al*., 1999), and they were confirmed by manual analysis of ^{15}N- and ^{13}C-3D NOESY spectra. Distance restraints were manually refined by iterative assignment corrections/structure calculations by using XPLOR-NIH (Schwieters *et al*., 2003). The assigned distance restraints were categorized in four classes for these calculations: I, <3.0 Å; II, <4.0 Å; III, <5.0 Å; and IV, <6.0 Å. Final structure calculations were based on a total of 1206 nuclear Overhauser effect (NOE)-derived interresidue distance restraints (class I, 10; II, 129; III, 318; and IV, 749), and 26 distance restraints mimicking H-bonds identified using characteristic short range NOE patterns (Table 1). All structures were subjected to a refinement in water by using XPLOR-NIH (Schwieters *et al*., 2003) and the parallhdg5.3 force fields (Linge *et al*., 2003). The final ensemble of 20 structures selected by lowest NOE energy showed the following distribution in the Ramachandran plot: 82.5% most favored, 12.8% additionally allowed, 2.3% generously allowed, and 2.5% disallowed. For analysis of the refined ensemble MOLMOL (Koradi *et al*., 1996), Procheck-NMR (Laskowski *et al*., 1996) were used. Structural information derived from an ensemble of 20 structures is shown in Table 1. Structural coordinates have been registered in Protein Data Bank (accession code: 2jp7).

Chromatin immunoprecipitation analysis, fluorescence in situ hybridization (FISH), and fluorescence titration experiments were performed as described in Gwizdek *et al*. (2006).

Table 1. NMR and refinement statistics for protein structures

	Protein
NMR distance and dihedral constraints	
Distance constraints	
Total NOE	1206
Intraresidue	4
Interresidue	1202
Sequential (|i-j| = 1)	432
Medium range (|i-j|<4)	429
Long range (|i-j| >4)	294
Ambiguous	47
Hydrogen bonds	26
Total dihedral angle restraints	0
Structure statistics	
Violations (mean ± SD)	
Distance constraints (Å)	0.0354 ± 0.0007
Maximum distance constraint violation (Å)	0.437
Deviations from idealized geometry	
Bond lengths (Å)	0.0171 ± 0.0003
Bond angles (°)	2.04 ± 0.04
Impropers (°)	2.3 ± 0.1
Avg. rmsd of 20 structures to the mean (Å)	
Heavy (ordered regions)	1.19 ± 0.16 (0.83 ± 0.13)
Backbone (ordered regions)	0.47 ± 0.11 (0.32 ± 0.10)

Surface Plasmon Resonance (SPR)

Quantitative interaction analyses were performed on a BIAcore 2000 instrument (BIAcore, Uppsala, Sweden). GST and GST-Hpr1 were amine-coupled to CM5 sensor chip to a density (R_L) of 2500 and 7000 resonance units (RUs), respectively. A mock-immobilized surface was used as a control. Coupling was performed using *N*-hydroxysuccinimide/*N*-(3-dimethylaminopropyl)-*N*′-ethylcarbodiimide reagents, ethanolamine, and HBS-EP buffer (10 mM HEPES, pH 7.5, 150 mM NaCl, 3 mM EDTA, and 0005% surfactant P20) (BIAcore). Binding experiments were performed in HSP-EP buffer at 25°C with 5 μM His-UBA-Mex67 as analyte in the mobile phase. The analyte was injected at a flow rate of 5 μl/min during 6 min alone or together with different concentrations of K48-linked tetraubiquitin. Specific sensorgrams were obtained after subtracting binding of the analyte to the mock-immobilized surface. After each run, surfaces were regenerated using 1 M NaCl, 50 mM NaOH. A control binding assay conducted after each round of regener-

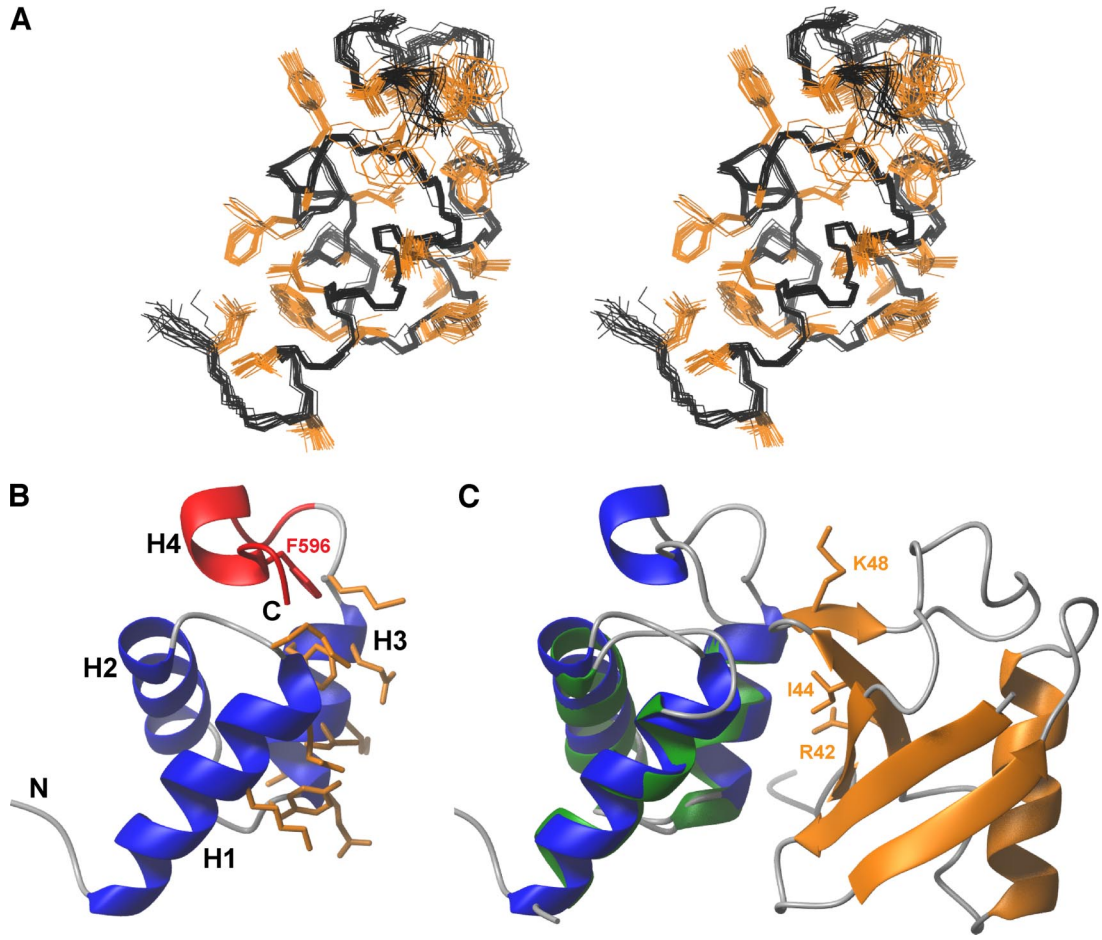

Figure 1. NMR structure of the Mex67 UBA domain and a model of its likely interaction interface with ubiquitin. (A) Stereo view of the ensemble of 20 NMR structures having the lowest total energy. Positions of the backbone-heavy atoms are given in black, whereas those of hydrophobic and aromatic side chains are in orange. (B) Representation of the secondary structure elements of the UBA-Mex67 closest to the mean of the NMR ensemble. The residues of UBA-Mex67 that may interact with monoubiquitin are in orange. The region of the structure deleted in UBAΔH4-Mex67 and Phe596 are highlighted in red. (C) Prediction of the likely docking geometry of the Mex67 UBA domain onto ubiquitin by analogy with the structure of the Ede1:ubiquitin complex (PDB:2G3Q). Ubiquitin is orange, and the Ede1 UBA domain is green. Helices H1-H3 of the UBA-Mex67 domain (blue) were superimposed on the corresponding helices in the Ede1 structure. The side chains of the key residues Lys48, Ile44, and Arg42 on ubiquitin are also shown in orange.

ation shows a reproducible response. Experimental equilibrium responses and R_{max} values were obtained using a "two-state reaction model with conformation change" (BIAevaluation software; BIAcore). Each experiment has been repeated at least twice.

RESULTS

Solution Structure of the Mex67UBA Domain

To elucidate the basis for the interaction of the Mex67 UBA domain with its partners, we obtained the solution NMR structure of the Mex67 UBA domain (Figure 1A) by using a set of 1232 structural restraints (Table 1), from which a well-defined ensemble of 20 structures was obtained that showed an average root mean square deviation (rmsd) to the mean structure of 0.47 Å for all backbone-heavy atoms, and an average rmsd to the mean structure of 1.19 Å when all heavy atoms were included. The structure contained four α-helices (residues 546–559 [H1], 563–572[H2], 578–586[H3], and 593–596[H4]) and overall, the fold is very similar to that of the TAP UBA domain (Grant *et al.*, 2002; 2003). In contrast to other UBA folds, the Mex67 UBA domain has an additional C-terminal helix (H4) that helps stabilize the core by burying hydrophobic side chains of helix H1 and loop 1 (Figure 1). The solution structures of the Mex67 and TAP UBA domains can be superimposed with rmsd of 1.4 Å, consistent with their sequence homology (Supplemental Figure 1).

UBA-Mex67 retains several features that in other UBA domains are involved in the interaction with ubiquitin. Thus, residues in both helix H1, loop1, and helix H3 have been reported to interact with ubiquitin in UBA:monoubiquitin complexes (Kang *et al.*, 2003; Mueller *et al.*, 2004; Ohno *et al.*, 2005). Analogous residues are present in Mex67, and they are exposed on the surface. These include the hydrophobic residues Tyr^{577}, Glu^{578}, Val^{579}, Ile^{581}, Lys^{582}, Phe^{584}, and Gln^{585} of helix H3 and Lys^{554} and Glu^{558} of the helix H1 (Figure 1C). Mex67 and TAP show a high degree of structural homology with the UBA domain of yeast Ede1 (Swanson *et al.*, 2006). The structures of the Mex67 and Ede1 UBA domains can be superimposed with rmsd of 1.13 Å, and many residues in either the hydrophobic core or binding to ubiquitin are conserved between these UBA domains (Figure 1C). However, in both Mex67 and TAP, loop 1 is

Table 2. In vitro measurement of dissociation constants of Mex67 and Rad23-derived GST and His6 fusion proteins of the respective UBA domains for mono- and Lys48-linked tetraubiquitin (K48-Ub4)

Recombinant protein	K_D for mono-Ub (μM)	K_D for K48-Ub4 (μM)
GST-UBA2-Rad23	19 ± 2	7.8 ± 1.2
His-UBA2-Rad23	12.9 ± 3.2	6.1 ± 0.2
GST-UBA-Mex67	400	>300
His-UBA-Mex67	400	>400
UBA-Mex67	Not determined	>300
GST-UBAΔH4-Mex67	63 ± 4	18 ± 2.4
UBA-Mex67(V597A)	Not determined	>300
UBA-Mex67(F596A)	Not determined	68 ± 5
His-UBA-Mex67:GST-Hpr1	Not detectable	7.5 ± 3
GST-Hpr1	No binding	No binding
GST-Mex67	12 ± 3	6.2 ± 0.6
GST-Mex67ΔUBA	300–400	300
GST-Mex67ΔH4	13 ± 2.1	3.7 ± 1.2

The association with ubiquitin was measured in vitro by monitoring the fluorescence enhancement of fluorescently labeled ubiquitin.

shorter than in other UBA folds and likely forms hydrophobic interactions with H4, suggesting that interaction with ubiquitin might be altered in the Mex67 UBA domain.

Helix H4 Influences the UBA-Mex67:Ubiquitin Interaction

Titrations using fluorescently labeled ubiquitin and recombinant UBA-Mex67 (Table 2) showed that, in contrast to UBA2-Rad23, UBA-Mex67 had low affinity (K_D = 400 μM) for monoubiquitin, regardless the tag used. However, deletion of H4 (UBAΔH4-Mex67) increased the affinity of UBA-Mex67 for monoubiquitin substantially (K_D = 63 μM), suggesting that the presence of helix H4 may impede the interaction with ubiquitin. Deletion of helix H4 allowed UBA-Mex67 to bind Lys48-linked tetraubiquitin with a slightly higher affinity than monoubiquitin (K_D = 18 μM). It should be noted that full-length Mex67 was able to interact with ubiquitin via its UBA domain, suggesting a conformational control of the UBA-Mex67 and H4 by other domains of the protein in vitro. However, deletion of H4 in the context of full-length Mex67 still increased by twofold the affinity of Mex67 for tetraubiquitin without affecting the K_D for monoubiquitin (Table 2). Consistently, pull-down experiments using GST-Mex67 or GST-Mex67ΔH4 and extracts from Δerg6 cells revealed that deletion of H4 improves to some extent the ability of Mex67 to interact with polyubiquitylated proteins (data not shown). We also investigated the effect of point mutations in helix H4 on the UBA-Mex67:ubiquitin interaction and found that, whereas UBA-Mex67(V597A) was indistinguishable from wild type, mutation of F596A (that faces and probably interacts with residues in loop 1 allowed binding to ubiquitin (K_D = 68 μM). Because the corresponding mutation in the TAP UBA domain (F617A) causes a conformational change in helix H4, these data should not be interpreted as indicating a direct involvement of Phe^{596} in preventing the interaction with ubiquitin but rather as a regulatory role on residues involved in ubiquitin binding (Grant *et al*., 2003).

Role of Helix H4 in the Interaction with Hpr1

Besides binding ubiquitin, the UBA-Mex67 UBA also interacts specifically with the C-terminal domain of Hpr1 (Gwizdek *et al*., 2006). GST-pull-down and two-hybrid assays both showed that the strength of the interaction of UBA-Mex67 with Hpr1 was greatly reduced by deletion of helix H4 (Figure 2, A and B) or by the F596A point mutation (Figure 2C), indicating that helix H4 is also important for the interaction with Hpr1. It was unlikely that this loss of function was associated with UBA-Mex67 being denatured by the removal of helix H4, because these mutants showed a gain of function in terms of affinity for ubiquitin.

The interaction between UBA-Mex67 and Hpr1 was also analyzed by SPR by using GST-Hpr1 as ligand and recombinant His-UBA-Mex67 or UBAΔH4-Mex67 as the mobile phase. Specific association and dissociation could be observed between GST-Hpr1 and UBA-Mex67 (2.5 μM) but not with GST alone (Figure 2D). Consistent with the GST-pull-down and two-hybrid assays, UBAΔH4-Mex67 bound GST-Hpr1 with much lower affinity. The best fits for UBA-Mex67 required a two-state reaction model that included a conformation change and not the classical 1:1 Langmuir model (BIAevaluation software; BIAcore). The kinetically determined K_D value of the UBA-Mex67:Hpr1 interaction was ~4 μM, whereas k_2 and k_{-2} corresponding to the conformation change were 6.5×10^{-3} and 10^{-3} s^{-1}, respectively (Table 3), consistent with there being a conformational change in the UBA-Mex67:Hpr1 complex following the initial binding.

Hpr1 Binding Facilitates the UBA-Mex67:Ubiquitin Interaction

These results prompted us to investigate whether Hpr1 binding altered the affinity of UBA-Mex67 for ubiquitin. Although the purified recombinant GST-Hpr1:His-UBA-Mex67 complex did not have measurable affinity for monoubiquitin, it clearly interacted with Lys48-linked tetraubiquitin with a K_D of 7.5 ± 3 μM, comparable with that observed for Rad23-UBA (Table 2). Consistently, we did not detect an interaction between GST-Hpr1:UBA-Mex67 neither with 1.4 nor 10 μM monoubiquitin by SPR (data not shown). However, when increasing concentrations of K48-linked tetraubiquitin (0–7 μM) were used in SPR studies together with 5 μM His-UBA-Mex67 for binding to immobililized GST-Hpr1, the signal increased fivefold in the presence of 7 μM ubiquitin, consistent with the formation of a GST-Hpr1:UBA-Mex67:tetraubiquitin tripartite complex and with every GST-Hpr1:UBA-Mex67 complex binding ubiquitin (Figure 3). Both the equilibrium RU values as well as the kinetically determined value of global K_D indicated that the K_D for the interaction between the GST-Hpr1:UBA-Mex67 complex and tetraubiquitin was in the micromolar range and so in reasonable agreement with the fluorescence titration data (Tables 2 and 3). In addition, k_2 and k_{-2}, corresponding to the putative conformation change after formation of the GST-Hpr1:UBA-Mex67 complex, were not altered by the presence of tetraubiquitin (Table 3). These results indicate that Hpr1 binding, likely followed by a conformational change, influences the binding of UBA-Mex67 to ubiquitin.

Deletion of Helix H4 Reduces Recruitment of Mex67 to mRNA In Vivo and Produces an mRNA Nuclear Export Defect

To confirm the contribution of H4 to the function of the UBA-Mex67 domain in vivo in the context of the full-length protein, we analyzed the consequences of deleting helix H4, by using yeast strains expressing HA-tagged-wild type Mex67 (Mex67-HA) or ΔH4-Mex67 (*mex67-ΔH4-HA*) that were generated from the MEX67 shuffle strain. Because binding of UBA-Mex67 results in the transient protection of ubiquitylated Hpr1 from

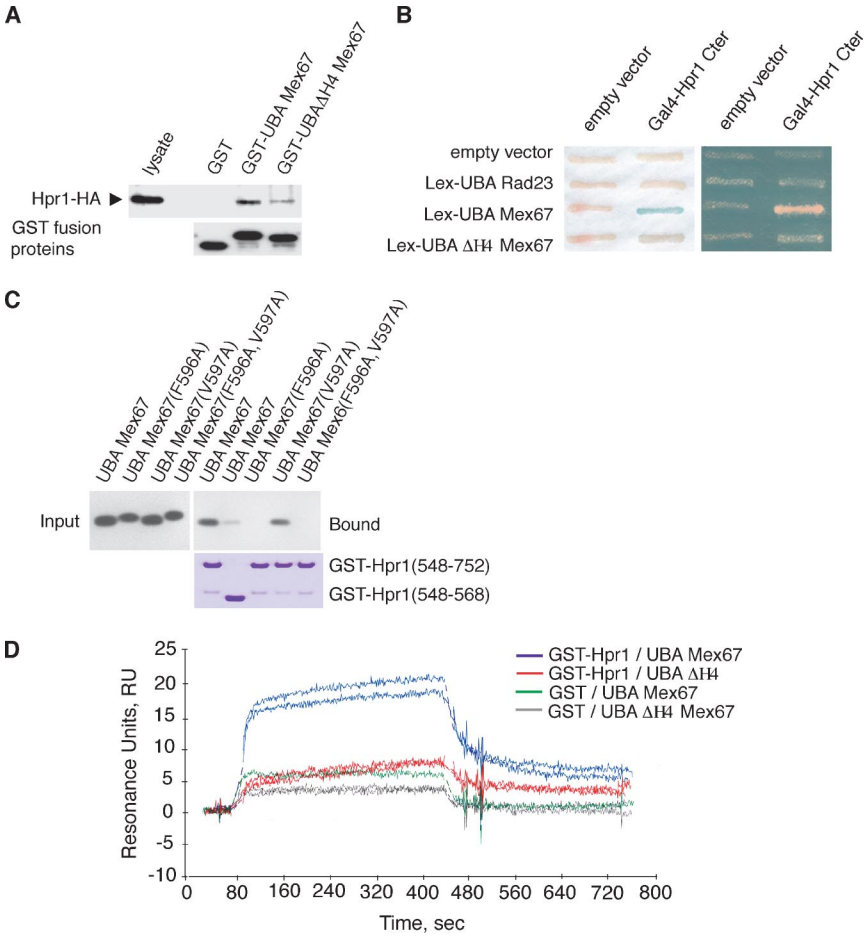

Figure 2. Role of helix H4 of the Mex67 UBA domain in its interaction with Hpr1. (A) Pull-down assays using indicated GST fusion recombinant proteins and lysates from cells expressing HA-tagged versions of Hpr1. (B) Two-hybrid analysis of the indicated LexA-fusion proteins versus Gal4-Hpr1 C terminus. Expression levels of wild-type and deletion mutant of UBA-Mex67 were analyzed by Western blotting and found to be similar. (C) Purified recombinant wild-type and mutant forms of UBA-Mex67 and indicated GST-Hpr1 fusion proteins were mixed (input) and complexes analyzed after purification on glutathione-Sepharose beads (bound) by Western blotting by using an anti-Mex67 antibody. (D) Duplicate SPR sensorgrams of the interaction between 2.5 μM His-UBA-Mex67 or UBAΔH4-Mex67 as analyte on amine-coupled GST or GST–Hpr1 surfaces. The kinetic fit was obtained using BIAcore 2000 BIAevaluation software (two-state reaction with conformation change).

proteasome-dependent degradation (Gwizdek *et al.*, 2006), the stability of Hpr1 was analyzed in both strains. Heat-induced degradation of Hpr1 was accelerated in *mex67-ΔH4-HA* compared with Mex67-HA cells (Figure 4A) consistent with the weak interaction observed between ΔH4-UBA-Mex67 and Hpr1 in vivo (Figure 2). Because the Mex67 UBA domain is required for both its recruitment to transcribing genes and mRNA nuclear export (Gwizdek *et al.*, 2006), we used chromatin immunoprecipitation analysis to assess the consequences of deleting helix H4 on Mex67 recruitment to active genes. Deletion of helix H4 in *mex67-ΔH4-HA* cells resulted in decreased cotranscriptional recruitment of Mex67 on *GAL10* (Figure 4B). As shown previously for deletion of the entire UBA domain, deletion of helix H4 did not influence recruitment of RNA polymerase II (CTD) to *GAL10*, consistent with helix H4 contributing to the recruitment of Mex67 to actively transcribing genes. Deletion of helix H4 did not affect the ability of Mex67-

Table 3. SPR measurements of the interaction of immobilized GST-Hpr1 with His-UBA-Mex67 as an analyte in the absence or in the presence of Lys48-linked tetraubiquitin (K48-Ub4)

Analyte	Apparent K_D (M)	R_{max} (RU)	k_2 (s^{-1})	k_{-2} (s^{-1})
UBA (5 μM)+				
0	3.7×10^{-6}	31	6.5×10^{-3}	9.9×10^{-4}
K48-Ub4 (1 μM)	4.3×10^{-6}	83	6.7×10^{-3}	9.8×10^{-4}
K48-Ub4 (3.5 μM)	5.0×10^{-6}	133	7.1×10^{-3}	12×10^{-4}
K48-Ub4 (7 μM)	6.1×10^{-6}	146	6.6×10^{-3}	9.0×10^{-4}

Apparent K_D corresponds to K_D of the interaction between GST-Hpr1 and UBA-Mex67 ± K48-Ub4 without considering the conformational change whose k_2 and k_{-2} are indicated separately. Data correspond to mean of at least two independent experiments.

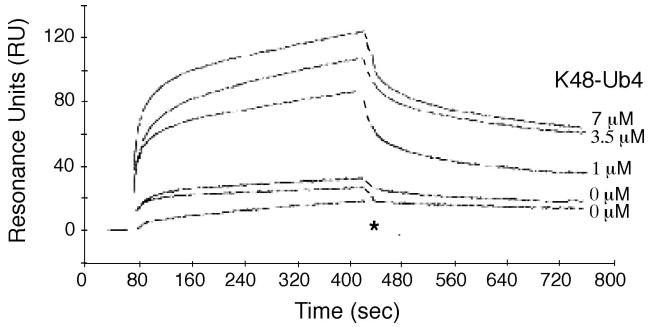

Figure 3. Tetraubiquitin binding to UBA-Mex67 requires interaction of the Mex67 UBA domain with Hpr1. SPR sensorgrams of interaction of 5 μM His-UBA-Mex67 with immobilized GST-Hpr1 in the absence or in the presence of increasing concentrations of Lys48-linked tetraubiquitin (K48-Ub4). The association of 1 μM Lys48-Ub4 with the GST–Hpr1 surface is shown as control (*). Interruption of association and dissociation curves due to alterations in refractive index during buffer changes were artificially filled with dashed lines.

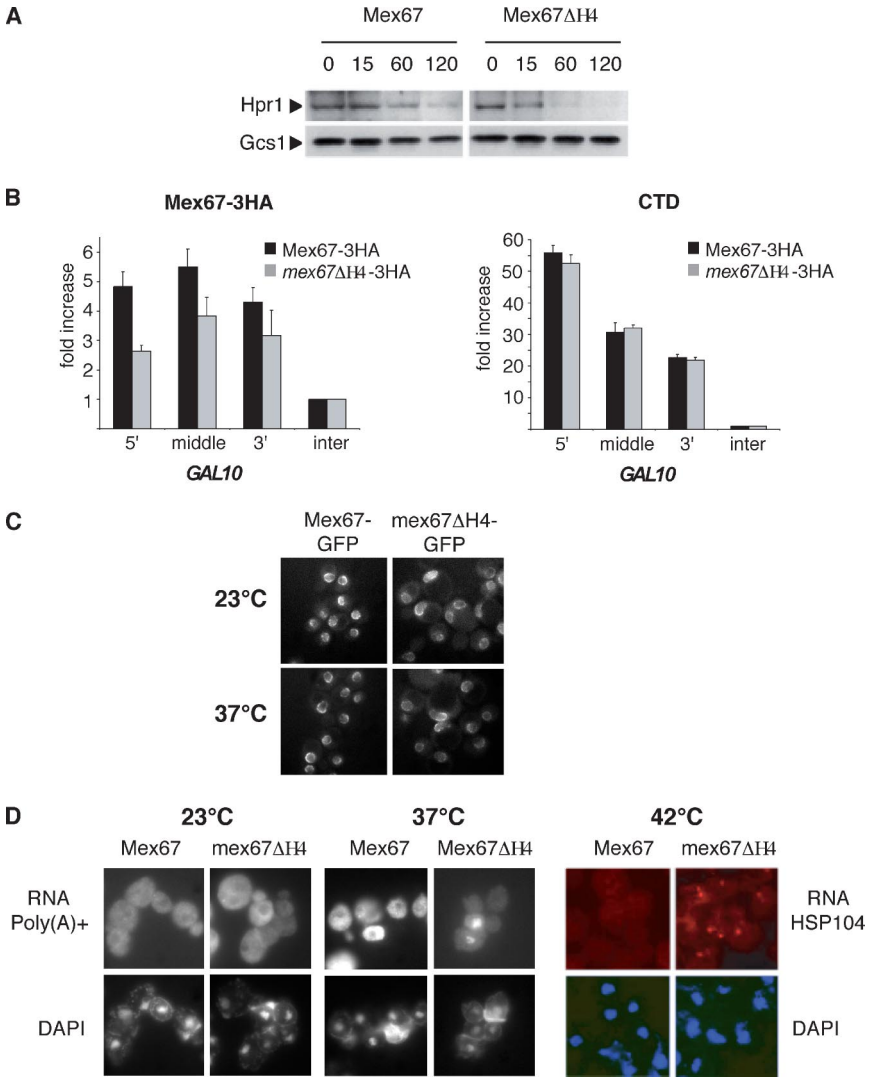

Figure 4. Role of helix H4 of the Mex67 UBA domain in cotranscriptional recruitment of Mex67 and mRNA export. (A) Steady-state level of Hpr1 expression was analyzed in Mex67-3HA and *mex67-ΔH4-3HA* cells shifted to 37°C for different incubation times. The Gcs1 protein was used as a loading control. (B) Chromatin immunoprecipitation experiments on *GAL10* were performed with extracts prepared from Mex67-3HA or *mex67-ΔH4-3HA* strains shifted to galactose for 2 h by using the anti-HA or anti-CTD antibodies. Significance of the differences observed for Mex67 recruitment between wild-type and mutant cells was evaluated using Student's *t* test. Values were found to be $p = 0.004$ for the 5′, $p = 0.02$ for the middle, and $p = 0.07$ for the 3′. (C) Subcellular localization of Mex67 was analyzed by direct green fluorescent protein (GFP) fluorescence on Mex67-GFP and *mex67ΔH4-GFP* cells. (D) Subcellular localization of poly(A)+ RNA was analyzed by FISH by using oligo(dT) Cy3 as probe in cells kept at 23°C or shifted to 37°C for 3 h (left). Alternatively, HSP104 mRNA was analyzed by FISH by using a specific probe in Mex67-3HA or in *mex67ΔH4-3HA* shuffle strains after a 30-min shift to 42°C (right).

GFP to localize at the nuclear pore complex in vivo (Figure 4C). However, absence of helix H4 resulted in lower levels of mRNA export when the distributions of poly(A)+ RNA or the specific *HSP104* transcript were examined in *mex67-ΔH4-HA* cells by FISH and compared with wild-type Mex67-HA cells (Figure 4D). In agreement with observations in *mex67-ΔUBA-HA* cells (Gwizdek *et al*., 2006), no poly(A)+ RNA export defect was detected at 23°C. However, 20% of *mex67-ΔH4-HA* cells accumulated poly(A)+ RNA in the nucleus after a 3-h shift at 37°C, whereas mRNA export was unaffected in wild-type cells. The export defect was more pronounced for *HSP104*, as these transcripts accumulated within a nuclear dot in 70% of mutant cells after a 30-min shift to 42°C. Thus, the weaker Mex67 cotranscriptional binding observed in *mex67-ΔH4-HA* cells was paralleled by an mRNA export defect. Overall, both deletion of helix H4 alone or deletion of the entire UBA domain produce similar mRNA nuclear export phenotypes consistent with helix H4 regulating at least some functions of the Mex67 UBA domain.

DISCUSSION

Our data show that helix H4 of the UBA domain of Mex67 influences its interaction with other partners in different ways. Thus, whereas in vitro deletion of helix H4 or the F596A mutation increases the affinity of the UBA domain for ubiquitin and ubiquitin multimers, it reduces the affinity for Hpr1. Moreover, deletion of helix H4 reduces both cotranscriptional recruitment of Mex67 to mRNPs and generates an mRNA export defect at 37°C.

It is unlikely that deletion of helix H4 results in a complete loss of structure of the UBA domain, because these constructs retain the ability to bind ubiquitin. Instead, helix H4 seems to be involved directly in Hpr1 binding, and the pronounced mRNA export defect seen in *mex67-ΔH4-HA* cells would be consistent with the Hpr1:Mex67UBA interaction being an important step in the overall export pathway. However, it seems unlikely that helix H4 alone can account for all of the effects seen with deletion of the entire UBA domain, because previous studies have, for example, shown a role for the intact domain in interacting with phenylalanine-glycine nucleoporins to facilitate translocation through nuclear pore complexes (Grant *et al*., 2003). Our results indicate that the core of the UBA domain (helices H1–H3) is responsible for ubiquitin binding, whereas H4 participates to Hpr1 binding and also seems to regulate the interaction of the Mex67 UBA domain with ubiquitin. It should be noted that although H4 is necessary for Hpr1 binding, it is

likely not sufficient for this interaction as suggested by the residues within the UBA domain that are affected upon Hpr1 binding in NMR spectra (our unpublished observations). Because both ubiquitin binding and Hpr1 stabilization are important for cotranscriptional recruitment and mRNA export, interfering with either UBA domain or H4 results in both cotranscriptional recruitment and mRNA export defects.

Based on these results, we hypothesize that, in vivo, helix H4 may function to coordinate the ubiquitin binding activity of the Mex67 UBA domain with recognition of specific substrates, in particular Hpr1, and also prevent binding to nonspecific substrates. Such a function would probably require a two-stage mechanism for the recognition of ubiquitinated Hpr1 by UBA-Mex67, with an initial helix H4-dependent binding of Hpr1 followed by an interaction with ubiquitins conjugated to Hpr1. This type of UBA-Mex67:ubiquitin interaction might also occur with other partners. Substrate specificity and ubiquitin linkage selectivity of UBA domains seem to be interdependent and do not exclusively rely on intrinsic properties of UBA domains, but rather they are precisely controlled by their molecular environment, as we show here for UBA-Mex67. For example, a specific interaction of the HIV-1 accessory protein Vpr with hHR23A-UBA1 domain involves loop 1 (Withers-Ward *et al*., 2000), whereas interaction of the N-terminal Ubiquitin-like domain of hHR23A with hHR23A-UBA1 modulates its selectivity for polyubiquitin linkage.

Comparison of the structure of the Mex67 UBA domain with the structures of other UBA:ubiquitin conjugates indicates that much of the interaction surface has been retained. For example, when the structure of the Mex67 UBA domain is superimposed on the UBA domain in the Ede1:ubiquitin complex (Swanson *et al*., 2006), much of the general character and structure of the interaction interface is retained for helix H3 (Figure 1). How might helix H4 influence the interactions? Steric hindrance seems unlikely, because in our model for the UBA-Mex67:monoubiquitin complex, helix H4 does not contact ubiquitin, although steric hindrance may possibly be important for binding of Lys48-linked ubiquitin multimers. Alternatively, previous studies have shown that the structure of the TAP-UBA domain is relatively plastic and mutations can introduce movements of helices H1, H2, and H3 that significantly alter interactions with other partners. Structural studies revealed that helix H4 in TAP-UBA is highly mobile and undergoes major conformational changes upon binding FXFG repeats or in the F617A mutant (Grant *et al*., 2003). This result, together with the involvement of helix H4 in the interaction with Hpr1, would be consistent with the conformational change observed by SPR being associated with a change in helix H4 being triggered by binding to Hpr1. However, a change in the overall structure of the UBA domain associated with its binding Hpr1cannot be formally excluded. In either case, the conformational change induced by Hpr1 would facilitate ubiquitin binding by the UBA domain.

Although further work will be required to define the precise manner in which helix H4 modulates the interactions of the Mex67 UBA domain, our present studies demonstrate how the binding of Hpr1 can influence the affinity of this domain for ubiquitin and thereby provide a novel mechanism by which interactions between different components of the mRNP processing and export machinery can be modulated.

ACKNOWLEDGMENTS

We thank E. Hurt (Heidelberg University, Germany) and A. Jacquier (Institut Pasteur, Paris, France) for reagents and J. M. Camadro and B. Gontero-Meunier for help with SPR. This study was funded by grants from the Ministèrede la Recherche (ACI BCMS), Agence Nationale pour la Recherche grant BLAN06-1_134099 (to C.D.), the Ligue contre le Cancer (Equipe labelisée), Swiss National Science Foundation grant 102235 (to F.S.), and the Canton de Genève. M.H. is supported by the Ministèredélégué à la Recherche and holds a European Molecular Biology Organization short-term fellowship. C.B. holds a Federation of European Biochemical Societies postdoctoral fellowship.

REFERENCES

Clore, G. M., and Gronenborn, A. M. (1992). Application of three- and four-dimensional heteronuclear NMR spectroscopy to protein structure determination. Progress in Nuclear Magnetic Resonance Spectroscopy *23*, 43–92.

Cornilescu, G., Delaglio, F., and Bax, A. (1999). Protein backbone angle restraints from searching a database for chemical shift and sequence homology. J. Biomol. NMR *13*, 289–302.

Duncan, K., Umen, J. G., and Guthrie, C. (2000). A putative ubiquitin ligase required for efficient mRNA export differentially affects hnRNP transport. Curr. Biol. *10*, 687–696.

Grant, R. P., Hurt, E., Neuhaus, D., and Stewart, M. (2002). Structure of the C-terminal FG-nucleoporin binding domain of Tap/NXF1. Nat. Struct. Biol. *9*, 247–251.

Grant, R. P., Neuhaus, D., and Stewart, M. (2003). Structural basis for the interaction between the Tap/NXF1 UBA domain and FG nucleoporins at 1A resolution. J. Mol. Biol. *326*, 849–858.

Grzesiek, S., and Bax, A. (1992a). An efficient experiment for sequential backbone amide assignment of medium sized isotopically enriched proteins. J. Magn. Reson. *99*, 201–207.

Grzesiek, S., and Bax, A. (1992b). Correlating backbone amide and sidechain resonances in proteins by multiple triple resonance NMR. J. Am. Chem. Soc. *115*, 11620–11621.

Gwizdek, C., Hobeika, M., Kus, B., Ossareh-Nazari, B., Dargemont, C., and Rodriguez, M. S. (2005). The mRNA nuclear export factor Hpr1 is regulated by Rsp5-mediated ubiquitylation. J. Biol. Chem. *280*, 13401–13405.

Gwizdek, C., Iglesias, N., Rodriguez, M. S., Ossareh-Nazari, B., Hobeika, M., Divita, G., Stutz, F., and Dargemont, C. (2006). Ubiquitin-associated domain of Mex67 synchronizes recruitment of the mRNA export machinery with transcription. Proc. Natl. Acad. Sci. USA *103*, 16376–16381.

Hajduk, P. J., Meadows, R. P., and Fesik, S. W. (1997). Discovering high-affinity ligands for proteins. Science *278*, 497–499.

Harper, J. W., and Schulman, B. A. (2006). Structural complexity in ubiquitin recognition. Cell *124*, 1133–1136.

Hicke, L., Schubert, H. L., and Hill, C. P. (2005). Ubiquitin-binding domains. Nat. Rev. Mol. Cell Biol. *6*, 610–621.

Kang, R. S., Daniels, C. M., Francis, S. A., Shih, S. C., Salerno, W. J., Hicke, L., and Radhakrishnan, I. (2003). Solution structure of a CUE-ubiquitin complex reveals a conserved mode of ubiquitin binding. Cell *113*, 621–630.

Kay, L. E., Ikura, M., and Bax, A. (2002). Proton-proton correlation via carbon-carbon coupling: a three-dimensional NMR approach for the assignment of aliphatic resonances in proteins labeled with carbon 13. J. Am. Chem. Soc. *112*, 888–889.

Koradi, R., Billeter, M., and Wüthrich, K. (1996). MOLMOL a program for display and analysis of macromolecular structures. J. Mol. Graph. *14*, 51–55.

Laskowski, R. A., Rullmannn, J. A., MacArthur, M. W., Kaptein, R., and Thornton, J. M. (1996). AQUA and PROCHECK-NMR: programs for checking the quality of protein structures solved by NMR. J. Biomol. NMR *8*, 477–486.

Liker, E., Fernandez, E., Izaurralde, E., and Conti, E. (2000). The structure of the mRNA export factor TAP reveals a cis arrangement of a non-canonical RNP domain and an LRR domain. EMBO J. *19*, 5587–5598.

Linge, J. P., Williams, M. A., Spronk, C. A., Bonvin, A. M., and Nilges, M. (2003). Refinement of protein structures in explicit solvent. Proteins *50*, 496–506.

Mueller, T. D., Kamionka, M., and Feigon, J. (2004). Specificity of the interaction between ubiquitin-associated domains and ubiquitin. J. Biol. Chem. *279*, 11926–11936.

Neumann, S., Petfalski, E., Brugger, B., Grosshans, H., Wieland, F., Tollervey, D., and Hurt, E. (2003). Formation and nuclear export of tRNA, rRNA and mRNA is regulated by the ubiquitin ligase Rsp5p. EMBO Rep. 4, 1156–1162.

Ohno, A., Jee, J., Fujiwara, K., Tenno, T., Goda, N., Tochio, H., Kobayashi, H., Hiroaki, H., and Shirakawa, M. (2005). Structure of the UBA domain of Dsk2p in complex with ubiquitin molecular determinants for ubiquitin recognition. Structure *13*, 521–532.

Pickart, C. M., and Eddins, M. J. (2004). Ubiquitin: structures, functions, mechanisms. Biochim. Biophys. Acta *1695*, 55–72.

Raasi, S., Varadan, R., Fushman, D., and Pickart, C. M. (2005). Diverse polyubiquitin interaction properties of ubiquitin-associated domains. Nat. Struct. Mol. Biol. *12*, 708–714.

Rodriguez, M. S., Dargemont, C., and Stutz, F. (2004). Nuclear export of RNA. Biol. Cell *96*, 639–655.

Rodriguez, M. S., Gwizdek, C., Haguenauer-Tsapis, R., and Dargemont, C. (2003). The HECT ubiquitin ligase Rsp5p is required for proper nuclear export of mRNA in *Saccharomyces cerevisiae*. Traffic *4*, 566–575.

Schwieters, C. D., Kuszewski, J. J., Tjandra, N., and Marius, C. G. (2003). The Xplor-NIH NMR molecular structure determination package. J. Magn. Reson. *160*, 65–73.

Strasser, K., Bassler, J., and Hurt, E. (2000). Binding of the Mex67p/Mtr2p heterodimer to FXFG, GLFG, and FG repeat nucleoporins is essential for nuclear mRNA export. J. Cell. Biol. *150*(4), 695–706.

Swanson, K. A., Hicke, L., and Radhakrishnan, I. (2006). Structural basis for monoubiquitin recognition by the Ede1 UBA domain. J. Mol. Biol. *358*, 713–724.

Trempe, J. F., Brown, N. R., Lowe, E. D., Gordon, C., Campbell, I. D., Noble, M. E., and Endicott, J. A. (2005). Mechanism of Lys48-linked polyubiquitin chain recognition by the Mud1 UBA domain. EMBO J. *24*, 3178–3189.

Varadan, R., Assfalg, M., Haririnia, A., Raasi, S., Pickart, C., and Fushman, D. (2004). Solution conformation of Lys63-linked di-ubiquitin chain provides clues to functional diversity of polyubiquitin signaling. J. Biol. Chem. *279*, 7055–7063.

Varadan, R., Assfalg, M., Raasi, S., Pickart, C., and Fushman, D. (2005). Structural determinants for selective recognition of a Lys48-linked polyubiquitin chain by a UBA domain. Mol. Cell. *18*, 687–698.

Vranken, W. F. *et al*. (2005). The CCPN data model for NMR spectroscopy: development of a software pipeline. Proteins *59*, 687–696.

Withers-Ward, E. S., Mueller, T. D., Chen, I. S., and Feigon, J. (2000). Biochemical and structural analysis of the interaction between the UBA(2) domain of the DNA repair protein HHR23A and HIV-1 Vpr. Biochemistry *39*, 14103–14112.